European Journal of Pharmaceutics and Biopharmaceutics 194 (2024) 74–84

Contents lists available at ScienceDirect

European Journal of Pharmaceutics and Biopharmaceutics

journal homepage: www.elsevier.com/locate/ejpb

Research paper

Enzymatic degradation pattern of polysorbate 20 impacts interfacial properties of monoclonal antibody formulations

Kathrin Gregoritza [a,*], Christos Theodorou [a], Marc Heitz [a], Tobias Graf [b], Oliver Germershaus [c], Manuel Gregoritza [d]

[a] Pharmaceutical and Processing Development, Pharma Technical Development Biologics Europe, F. Hoffmann-La Roche Ltd, Basel, Switzerland
[b] Analytical Development and Quality Control, Pharma Technical Development Biologics Europe, Roche Diagnostics GmbH, Penzberg, Germany
[c] Institute for Pharma Technology, School of Life Sciences, University of Applied Sciences and Arts Northwestern Switzerland, Muttenz, Switzerland
[d] Analytical Development and Quality Control, Pharma Technical Development Biologics Europe, F. Hoffmann-La Roche Ltd, Basel, Switzerland

ARTICLE INFO

Keywords:
Surfactants
Polysorbate
Surface tension
Interfacial properties
Antibody aggregation
Particles
Fatty acids

ABSTRACT

Polysorbate 20 (PS20) is widely used to maintain protein stability in biopharmaceutical formulations. However, PS20 is susceptible to hydrolytic degradation catalyzed by trace amounts of residual host cell proteins present in monoclonal antibody (mAb) formulations. The resulting loss of intact surfactant and the presence of PS20 degradation products, such as free fatty acids (FFAs), may impair protein stability. In this study, two hydrolytically-active immobilized lipases, which primarily targeted either monoester or higher-order ester species in PS20, were used to generate partially-degraded PS20. The impact of PS20 degradation pattern on critical micelle concentration (CMC), surface tension, interfacial rheology parameters and agitation protection was assessed. CMC was slightly increased upon monoester degradation, but significantly increased upon higher-order ester degradation. The PS20 degradation pattern also significantly impacted the dynamic surface tension of a mAb formulation, whereas changes in the equilibrium surface tension were mainly caused by the adsorption of FFAs onto the air–water interface. In an agitation protection study, monoester degradation resulted in the formation of soluble mAb aggregates and proteinaceous particles, suggesting that preferential degradation of PS20 monoester species can significantly impair mAb stability. Additional mAbs should be tested in the future to assess the impact of the protein format.

1. Introduction

Formulation composition and excipient stability are crucial to ensure safety and efficacy of therapeutic proteins. A main risk factor that can impair the stability of proteins is the exposure to interfaces [1–6]. In particular, air–water, water-container and water-silicone oil interfaces constitute a major risk for interfacial stress and protein adsorption. Upon interfacial stress, proteins may also undergo conformational changes that promote self-aggregation [7], which can affect quality, efficacy and safety of protein drugs [8,9]. Hence, the protection of the drug product against interfacial adsorption is of utmost importance. It is, therefore, imperative to use stabilizing surfactants. Non-ionic surfactants such as polysorbate 20 (PS20) and polysorbate 80 (PS80) are widely used as excipients in biopharmaceutical formulations due to their low toxicity and excellent biocompatibility. Polysorbates (PSs) protect and stabilize therapeutic proteins against above-mentioned interfacial stress, protein self-association and aggregation [3,10,11]. PSs protect and stabilize biopharmaceuticals by two mechanisms: PSs can bind to hydrophobic protein patches, which results in steric stabilization and enhanced solubilization, thereby preventing protein–protein association and

Abbreviations: CAD, charged aerosol detection; CALB, candida antarctica lipase B; CHO, chinese hamster ovary; CMC, critical micelle concentration; ELSD, evaporative light scattering detector; FFA, free fatty acid; FTIR, Fourier-transform infrared spectroscopy; HCPs, host cell proteins; HMWS, high molecular weight species; HOE, higher-order esters; HPLC, high performance liquid chromatography; ID, identification; LA, lauric acid; LC-MS, liquid chromatography - mass spectrometry; MA, myristic acid; NPN, N-phenyl-1-naphtylamine; OA, oleic acid; PA, palmitic acid,; PES, polyethersulfone; Ph.Eur, European Pharmacopeia; POE, polyoxyethylene; PS, polysorbate; PS20, polysorbate 20; PS80, polysorbate 80; RP-UPLC, reversed phase ultra performance liquid chromatography; SA, stearic acid; SEC, size exclusion chromatography; SR, super refined; USP, United States Pharmacopeia.

* Corresponding author at: Pharma Technical Development Biologics Europe, F. Hoffmann-La Roche Ltd., Grenzacherstrasse 124, Basel 4070, Switzerland.
E-mail address: kathrin.gregoritza@roche.com (K. Gregoritza).

https://doi.org/10.1016/j.ejpb.2023.11.024
Received 19 October 2023; Received in revised form 25 November 2023; Accepted 27 November 2023
Available online 30 November 2023

protecting against interfacial adsorption, respectively. PSs can also saturate the air-solution interface, thereby preventing interfacial adsorption of proteins and subsequent conformational changes [10]. It is important to note that commonly-used types of PS are highly heterogeneous mixtures with regard to fatty acid ester composition, as well as to their level of esterification. Specifications for fatty acid ester distributions are defined by the European Pharmacopeia (Ph. Eur.) and the United States Pharmacopeia (USP) with laurate esters being the main PS20 component at 40–60 %, followed by myristate and palmitate esters at 14–25 % and 7–15 %, respectively [12,13]. By contrast, no compendial specifications apply to the ratio of monoesters to higher-order esters (HOE) in PS.

Currently the topic of PS degradation and its impact on biopharmaceutical formulations is receiving high attention, in particular from the pharmaceutical industry [14–16]. Numerous studies have been published investigating the quality impact of PS degradation over product shelf life [17–25]. Oxidative and hydrolytic degradation pathways represent the main mechanisms leading to a variety of degradation products. For both mechanisms, the reduction of functional PS may impair the protein stabilizing properties of the surfactant. Oxidative degradation is enhanced by higher temperatures, light exposure, atmospheric oxygen, and raw material impurities such as peroxides [23,26–30]. Hydrolytic degradation is mainly promoted by process-related host cell proteins (HCPs) which can co-elute with therapeutic proteins during the downstream purification process. Even though HCPs are present in trace amounts, they can cause considerable hydrolytic cleavage of PS esters over shelf life [31–34], resulting in the release of free fatty acids (FFAs). Due to their hydrophobic nature and limited solubility, FFAs may accumulate and eventually precipitate, leading to the formation of sub-visible and visible particles [17,18,32,35]. A vast variety of PS-degrading enzymes has been identified and characterized regarding their hydrolytic activity and substrate specificity [31,33,34,36–39]. McShan and coworkers first reported that the PS degradation profile was unique to the type of enzyme used [39]. Based on these results, Graf et al. established a method for controlled enzymatic hydrolysis of PS20 [40]. By using different enzymes, including *Mucor miehei* lipase (MML) and *Candida antarctica* lipase B (CALB), distinct PS20 degradation profiles were achieved. MML preferentially cleaves di- and triesters, which are referred to as higher-order esters (HOE), whereas CALB preferentially cleaves the less bulky monoester species.

Although the protective effect of intact PS against interfacial stress of mAbs has been extensively investigated [41,42], little is known about the impact of PS subspecies degradation on surface tension and interfacial kinetic behaviors in biopharmaceutical formulations. Few studies have investigated the impact of isolated PS ester fractions on the colloidal protein stability. For example, Tomlinson et al. [24] and Diederichs et al. [43] have assessed the interfacial properties of isolated PS fractions, including sorbitan-POE-monoester, isosorbide-POE-monoester, and sorbitan-POE-multiesters, which were separated by preparative-scale high performance liquid chromatography (HPLC). It was found that these fractions possessed different critical micellar concentrations (CMCs) and surface tensions, as well as different capacities to protect model mAbs against interfacial stress. Although these studies provided essential insights into the surfactant-mediated stabilization of biopharmaceutical formulations, the use of isolated PS fractions bear little resemblance to the mixed conditions found in degraded PS20 formulations. Most recently, Glücklich et al. [44] studied how enzymatically hydrolyzed PS20 influences the stabilization of two model mAbs upon shaking stress using three different surrogate lipases. The results of those excellent studies and the findings of the present work will be compared and discussed later. The authors believe that looking at this complex topic from different angles using different model proteins and with different study designs is essential to ultimately understand the underlying processes.

The aim of the present study was to investigate the enzyme-catalyzed hydrolytic degradation of PS20 used in biopharmaceutical formulations and the resulting effects on protein-stabilizing properties in a particularly representative way by using partially hydrolyzed PS20 to mimic aged drug product conditions. In contrast to the abovementioned studies, we used bead-immobilized lipases to hydrolyze PS20 in a highly controlled manner. Two model lipases were selected - MML (HOE degradation) and CALB (monoester degradation) - because they yield two distinct PS20 degradation patterns. By using immobilized versions of these enzymes, partially degraded PS solutions with defined degradation profiles and levels were achieved. To investigate the impact of PS20 ester species on several critical surfactant properties, formulations comprising partially degraded PS20 with different degradation profiles (HOE vs. monoester degradation) were prepared and assessed for surface tension, interfacial parameters and CMC. Our findings provide an improved understanding of how the degradation pattern of PS20 impacts its stabilizing properties.

2. Materials and methods

2.1. Chemicals

Acetic Acid, Acetone, Brij35 (30 % w/v), Glutaraldehyde (25 % aqueous solution), Lauric-d_{23} acid, Lipase from *Mucor miehei* (4307 U/mg), Lipase B from *Candida antarctica* (7.9 U/mg), L-Methionine, L-Histidine, Myristic-d_{27} acid, N-phenyl-1-naphtylamine (NPN), Phosphate buffered saline tablets and Sucrose were purchased from Sigma-Aldrich (St. Louis, MO, USA), Ammonium acetate, Potassium chloride, Potassium dihydrogen phosphate, Methanol LiChrosolv, LC-MS Grade were obtained from Merck KGaA (Darmstadt, Germany), Formic acid 99 % was received from VWR International (Radnor, PA,USA). Glycine was obtained from Ajinomoto Co. LTD (Chūō, Japan). Di-potassium hydrogen phosphate was purchased from AppliChem GmbH (Darmstadt, Germany). Super refined PS20 (SR PS20) was provided by Croda International Plc. (Snaith, England). ReliZymeTM HA403/M was obtained from Resindion S.R.L. (Binasco, Italy). Sodium chloride and Tris (hydroxymethyl)aminomethane (TRIS) were purchased from Fisher Scientific (Hampton, VA, USA). mAb1 and mAb2 formulated at 10 mg/mL in histidine buffer pH 5.5, containing other stabilizing excipients were provided by F. Hoffmann-La Roche Ltd (Basel, Switzerland).

2.2. Methods

2.2.1. Immobilization of selected lipases on ReliZyme™ beads support

Enzymes were covalently linked to amine-modified polymethacrylate beads according to a procedure described by Graf et al. [40]. In brief, ReliZyme™ HA403/M beads were activated with 10 % glutaraldehyde solution for 14 h at ambient temperature and subsequently washed with 1.25 M phosphate buffer pH 7.0 to remove excess glutaraldehyde. Selected lipases were dissolved in phosphate buffered saline pH 7.4 and added to the activated beads. The immobilization step was performed overnight at ambient temperature using a horizontal shaker. Excess free aldehyde groups on the resin were quenched with a 0.2 M glycine solution in phosphate buffered saline pH 7.5. Subsequently, the beads were thoroughly washed with ultrapure water, 20 mg/mL PS20 solution and 0.05 M potassium phosphate buffer pH 7.0. The immobilized lipase beads were stored in 0.05 M potassium phosphate buffer pH 7.0 at 2–8 °C until further use.

2.2.2. Hydrolytic degradation of PS20 by immobilized lipases

Two degradation levels were prepared for each degradation pattern (MML and CALB), i.e. a low degradation level with 20–25 % PS degradation and a high degradation level with 55–60 % PS20 degradation. For this purpose, immobilized lipases were added to a SR PS20 stock solution (50 mg/mL) and incubated at 25 °C under gentle agitation. The degradation time was determined according to a previously assessed degradation study (cf. Fig. S1). PS20 degradation was stopped by

separating the partially degraded PS20 stock solutions from the lipase beads. The supernatant was transferred into 10 mL borosilicate type I glass vials and stored at 2–8 °C until used.

The content of intact PS20 was verified by mixed-mode high performance liquid chromatography (HPLC) coupled to an evaporative light scattering detector (ELSD) [45,46], whereas the composition of PS was assessed using reversed phase ultra performance liquid chromatography (RP-UPLC) coupled with charged aerosol detection (CAD) [47]. Peak areas of different PS20 fractions in the CAD chromatograms (non-esterified, mono-esterified, multi-esterified components) were used to calculate the ratio of HOE to total ester. The content of lauric acid (LA), myristic acid (MA), palmitic acid (PA) and stearic acid (SA) resulting from enzymatic PS degradation was quantified by liquid chromatography - mass spectrometry (LC-MS) [48]. Multiple partially degraded PS20 batches were prepared from the same PS20 SR raw material and the same batch of enzyme-beads. Each batch was separately tested for PS20 content.

2.2.3. Determination of critical micelle concentration (CMC) by N-Phenyl-1-Napthylamine (NPN) assay

CMCs of partially degraded PS solutions were determined using the fluorescent dye N-phenyl-1-naphthylamine- (NPN), which shows an increased fluorescence quantum yield when being exposed to an apolar environment [49]. The CMC determination assay was performed by preparing 2-fold serial dilutions of intact or degraded PS20 stock solutions in an assay buffer comprising 5 µM NPN, 50 mM TRIS, 0.15 M sodium chloride, 5 % acetonitrile and 15 ppm Brij35 at pH 8.0. Samples were transferred into opaque 384-well plates and analyzed in a Molecular Device Spectramax M2/M2e fluorescence plate reader. The excitation and emission wavelengths were set to 350 nm and 420 nm, respectively. The onset of fluorescence emission [24,49] as well as the inflection points of the Boltzmann fitted curves [50] were used to determine the CMCs.

2.2.4. Preparation and analysis of mAb formulations

Two CHO-derived IgG1 monoclonal antibodies (mAbs), referred to as mAb1 and mAb2, were produced in-house (Roche Diagnostics GmbH, Penzberg, Germany). mAb1 and mAb2 were formulated in a histidine buffer at pH 5.5, supplemented with sucrose and L-methionine. Corresponding placebo buffers were prepared and filtered with 0.22 µm polyethersulfone (PES) sterile filters prior to PS20 spiking. The nominal PS20 concentration in all sample formulations was 0.4 mg/mL, independent of the degradation level. Antibody formulations were prepared at 10 mg/mL for surface tension measurements and at 1 mg/mL for agitation stress studies. The protein content was verified by UV slope spectroscopy.

2.2.5. Equilibrium surface tension by pendant drop method

The equilibrium surface tension was determined by a pendant drop method using the PAT-1 M tensiometer (SINTERFACE Technologies, Berlin, Germany). Images of the drop profiles were captured by a CMOS-camera, and the software analyzed the droplet profiles by solving the Young-Laplace equation to obtain the interfacial area and the surface tension. During the course of the measurement, the droplet was permanently kept at a constant volume and apparent area as detected by the CMOS camera. This initial droplet area was chosen to ensure a pendant drop profile and to prevent the droplet from falling during the equilibration and oscillation. Therefore, the droplet volume decreased with increasing concentration of PS and/or degree of degradation (i.e. inducing lower surface tension and derived smaller drop volume needed for falling) which ranged from 22 to 29 mm^2. The measurements were carried out in duplicates and at room temperature (21–23 °C). The surface tension values were recorded every 5 s within the 20 min measurements and the surface tension at quasi-equilibrium was calculated as the average of the measurements between 19 and 20 min. The tubing system was rinsed with 1 mL of sample solution between each duplicates and with approximately 5 mL buffer solution between the samples to avoid any contamination. Samples measured were the above described intact or degraded PS solutions or some produced in purpose for the spiking experiments. These spiking solutions of PS20 and LA at different molar ratios were performed as previously published [17] by solubilizing LA into pure PS20 (at ratios PS20/LA of 1.0/0.0 to 0.0/1.0) and then diluted in 20 mM histidine buffer at pH 6.0 to the desired concentrations. The buffer exchange was performed with the same device, only using a coaxial needle from which, after an equilibration of 1 h, the same buffer without PS20 or LA was gradually exchanged at a rate of 0.5 µL/s for 7 h. Results of the spiking and buffer exchange experiment can be found in the supplementary information.

2.2.6. Dynamic surface tension by maximum bubble pressure method

For the investigation of interfacial kinetic behavior of samples containing either intact or degraded PS20 the maximum bubble pressure method was used. Using the bubble pressure tensiometer BP50 (Krüss GmbH, Hamburg, Germany), surface tensions at surface ages ranging from 15 to 5000 ms could be assessed. Investigated mAb and placebo formulations at pH 5.5 were spiked with either intact PS20, or PS20 partially degraded by CALB and MML (low and high degradation level) and were measured in duplicates at room temperature (23–25 °C). Solutions comprising either mAb1 or mAb2 at 10 mg/mL in formulation buffer without surfactant were used as references. Pressure probe and pipette tip were directly inserted into the 6cc sample vial. Calibration was conducted by using a buffer solution containing neither PS20 nor mAb.

2.2.7. Stress studies with mAb1 formulations containing partially degraded PS20

Partially degraded PS solutions were tested for their residual ability to protect the antibody from surface induced aggregation using an agitation study. mAb1 formulated at 1.0 mg/mL in histidine buffer at pH 5.5, stabilized with sucrose and L-methionine, was spiked with either partially degraded or intact PS20 at a nominal concentration of 0.4 mg/mL. Samples were incubated for 30 min at 30 °C to bring any insoluble FFAs into solution and filtered through 5 µm PES membrane filters to remove any extrinsic particles. 2.7 mL of filtered sample solutions were filled into 6 cc borosilicate type I glass vials and agitated on a horizontal shaker at 200 rpm for 1 week at 25 °C. Corresponding samples statically stored at 25 °C, as well as one unstressed initial control which was formulated with intact PS20 and subsequently stored at −80 °C, were used as controls. All formulations were prepared in triplicates.

2.2.8. Characterization of mAb1 samples

Following agitation or static storage at 25 °C, vials were visually inspected using a black/white panel according to Ph.Eur. 2.9.20 [51] and by enhanced visual inspection using a Seidenader V90-T semi-automated vial inspection machine (Seidenader Maschinenbau GmbH, Markt Schwaben, Germany). During the inspection with the Seidenader V90-T, vials were placed at an inclination of 61°, illuminated from the back, and rotated for 3 sec at 150 rpm prior to inspection through a 2-fold magnifying glass [52,53].

Sub-visible particles were quantified by light obscuration according to Ph.Eur. 2.9.19 [54] using a HIAC/ROYCO 9703 Liquid Syringe Sampler 3000A with a HRLD-150 sensor (Skan AG, Allschwil, Switzerland). Particles of selected samples were isolated on gold-coated polycarbonate filters (0.8 µm pore size) and characterized by Fourier-transform infrared spectroscopy (FTIR) using a Nicolet™ iNTM10 Infrared Microscope (Thermo Fisher Scientific, Reinach, Switzerland) by comparison to reference spectra. Soluble mAb aggregates were quantified as the sum area% of high molecular weight species (HMWS) by size exclusion chromatography (SEC) using a TSKgel SuperSW mAb HR HPLC (4 µm, 7.8 mm X 300 mm) column (Tosoh Bioscience) on a Waters Alliance 2695 HPLC system equipped with an UV/absorbance detector

(detection at 280 nm). Separation was performed at a constant oven temperature of 25 °C, using a mobile phase comprising 200 mM K_2HPO_4/KH_2PO_4 and 250 mM KCl, pH 6.2 at a flow rate of 0.35 mL/min. Visual inspection and sub-visible particle assessment was performed directly after completion of the study to avoid any temperature dependent particle nucleation, whereas samples were transiently stored at 2–8 °C prior to the HP-SEC analysis.

3. Results and discussion

Enzymatic hydrolysis of PS20 using immobilized enzymes.

PS20 was partially hydrolyzed using two different model lipases, CALB and MML, which possess different specificities against monoester and HOE-species in PS20. While CALB mainly degrades mono-esterified components, MML primarily targets multi-esterified species. In order to control the extent of degradation, CALB and MML were immobilized onto beads according to a method described by Graf and coworkers [40]. Respective enzyme beads were incubated with PS20 stock solutions and removed once the target PS20 degradation levels were reached (cf. Fig. S1).

As shown in Fig. 1 the specificity of CALB and MML towards their preferred substrate was higher at 20–25 % degradation (representing low degradation level). Once the preferred substrates had been consumed (at the high degradation level of 55–60 %), enzymes proceeded to degrade less preferred substrates, i.e., HOE for CALB and monoester species for MML. This observation was also reflected by the calculated ratios of HOE to total esters (Fig. 2), in which values >0.5 indicate preferential monoester degradation and values <0.5 indicate preferential HOE degradation, correspondingly. For PS20 samples degraded by CALB, the multi ester to total ester ratio steeply increased until a degradation level of 30 % was reached, this was followed by a plateau (30–50 % degradation) and then finally a decrease above 50 % degradation. By contrast, for PS20 samples degraded by MML, the multi-ester to total ester ratio continuously decreased until a degradation level of 50 % was reached and then a plateau was observed. The specificity of CALB towards the preferred substrate (monoesters) was slightly higher as compared to MML (preferred substrate: HOE) which was indicated by a steeper slope of the multi to total ester ratio of samples degraded by CALB (Fig. 2), as well as by the respective shallow gradient degradation profiles (Fig. 1).

In general, higher-order esters can be converted to monoester species [26], which is often indicated by an initial increase in peak area of

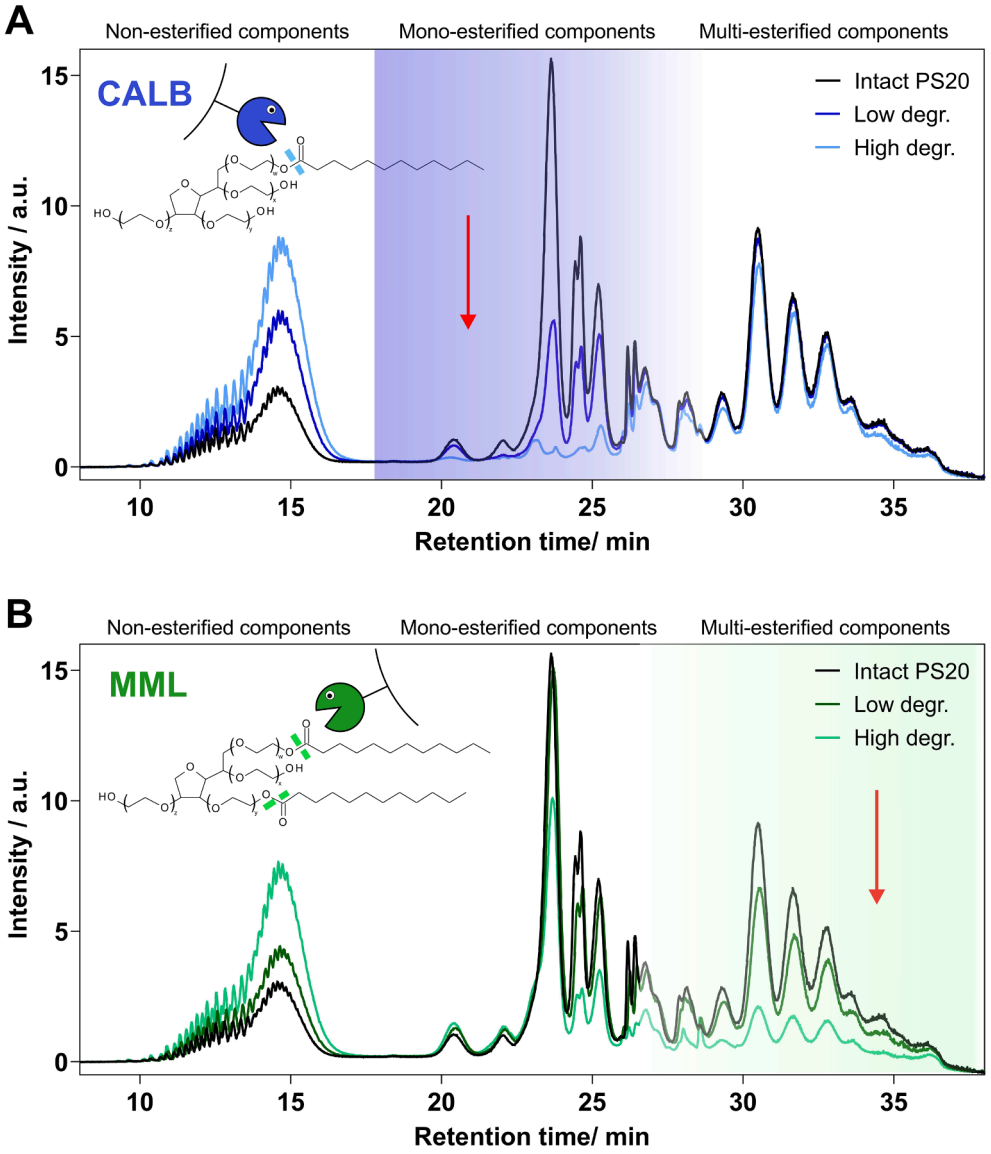

Fig. 1. RP-UPLC-CAD chromatograms of PS20 partially degraded by (A) CALB or (B) MML, comprising low degradation (20–25%) and high degradation (55–60%) preparations as well as intact PS20 (reference).

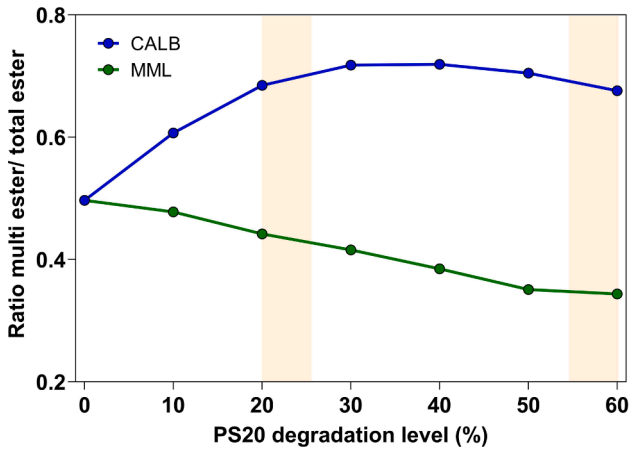

Fig. 2. HOE to total ester ratios of PS samples degraded by CALB and MML. Peak areas of different PS20 fractions in the CAD chromatograms (non-esterified, mono-esterified, multi-esterified components) were used to calculate the ratio of HOE to total esters. Highlighted ranges indicate the two degradation levels used in this study.

mono-esterified species. Using immobilized MML, only a minor increase in peak area was observed for two peaks eluting at 20–20.5 min which suggests that immobilized MML does not only degrade HOE into monoester, but continues hydrolyzing monoesters into POE as the substrate is already in close proximity to the active center of the enzyme. This effect might be caused by the high avidity and multivalency of MML-decorated beads and is expected to be different if soluble enzymes are used.

It needs to be noted that the HOE to total ester ratios were determined based on the relative area% in the CAD chromatograms and not quantified against reference standards, which would provide a more precise estimate of the PS ester distribution.

Critical micellar concentration (CMC).

The impact of the different enzymatic routes of PS degradation on the CMC was assessed using the fluorescent probe NPN, which fluoresces once incorporated into the apolar core of micelles and shows a 10-fold decreased quantum yield in an aqueous environment [24,49]. The CMC describes the concentration of amphiphilic molecules above which micelles are formed in solution and can be either assessed as the onset of fluorescence emission [24,49] or the inflection point of the curve [50]. In general, a lower CMC indicates a lower risk for FFA particles as lower concentrations of the surfactant are needed to form micelles that can

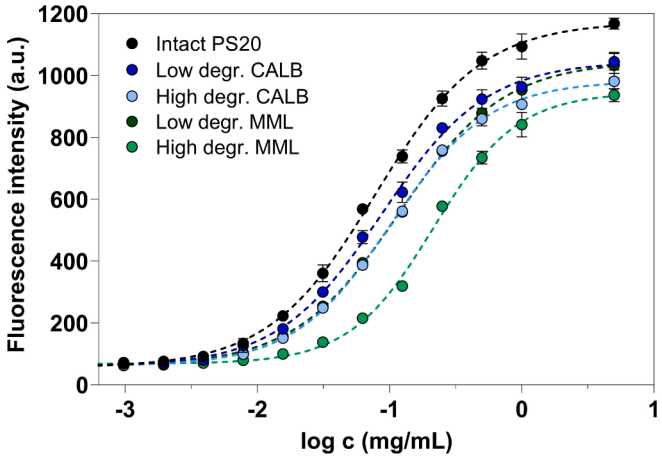

Fig. 3. CMC determination for intact and partially degraded PS20 (after treatment with CALB or MML). Corresponding value of fluorescence onset and IC50 reported in Table S1.

encapsulate insoluble FFAs and, consequently, reduce the concentration of FFAs in solution.

Fig. 3 depicts the NPN fluorescence intensity as a function of total PS20 concentration (degraded + undegraded). Intact PS20 showed the highest maximum fluorescence (at high PS20 concentrations), as well as the lowest CMC, which was expected since intact PS20 is essential for the formation of micelles and its ability to form micelles is diminished upon enzymatic hydrolysis.

Interestingly, the maximum fluorescence intensity of the curves was not only impacted by the overall degradation level but also the enzymatic degradation pattern, with PS20 degraded by MML showing the lowest fluorescence intensity independent of the degradation level. At the same time, the CMC increased with a higher PS20 degradation level, with the extent of CMC increase dependent on the employed lipase. MML-degraded samples showed a significantly higher increase in CMC compared to CALB-degraded samples at similar degradation levels, suggesting that the more hydrophobic PS20 multi-ester components can form micelles more readily. These observations indicate, that multi-ester degradation poses a higher risk for FFA particle formation, as these PS subspecies can form micelles and encapsulate FFAs more efficiently than corresponding monoesters, and are in line with two recently published studies: Tomlinson et al. [24] have investigated the physicochemical properties of fractionated PS20 esters and found that the CMC decreased with increasing hydrophobicity of the PS20 tail groups (i.e. sorbitan-POE-dilaurate > (isosorbide-)POE-monolaurate > sorbitan-POE-monolaurate). Micellation of PS in aqueous solution is a thermodynamic process which involves the dehydration and subsequent aggregation of the lipophilic tail groups of PS into micellar structures [55]. Both steps are thermodynamically favored for the more hydrophobic HOE compared to the corresponding monoesters. Lapelosa and coworkers [56] have used molecular simulations to assess the micellar aggregation behavior of PS20 ester fractions. Simulations of the sorbitan dilaurate and sorbitan monolaurate revealed a similar radius of gyration (22 Å). However, the hydrophobic effect was significantly stronger for the sorbitan dilaurate, resulting in a faster assembly of surfactant molecules into micelles (20 ns instead of 50 ns), as well as a denser core of the sorbitan dilaurate micelles. The free energy of interaction between sorbitan dilaurate molecules was determined to be significantly larger compared to that of sorbitan monolaurate.

Interfacial properties of partially degraded polysorbate in mAb formulations.

Equilibrium surface tension measurements were conducted using the pendant drop method. Each sample was recorded over a 1200 s (20 min) time frame to allow the surface tension to reach equilibrium. As shown in Fig. 4, no significant differences between mAb-containing solutions and corresponding placebos were observed, suggesting that the interface was efficiently protected by the surfactant, preventing the adsorption of mAb molecules.

The equilibrium surface tension in all samples was gradually decreased with increasing PS20 degradation, ranging from 37.5 ± 0.2 mN/m (intact PS20) to 26.0 mN/m for CALB-degraded samples and to 27.0 mN/m for MML-degraded samples, indicating that the resulting FFAs are surface active and can accumulate at the water–air interface. Doshi et al. [57] have hypothesized that FFAs can either co-adsorb onto the liquid–air interface, resulting in the partial displacement of PS20 molecules from the surface, or the formation of a more tightly packed mixed-layer of PS and FFA molecules.

To assess the impact of FFAs on the equilibrium surface tension in the presence of different levels of intact PS20, a spiking study was performed (Fig. S2). Increasing levels of LA, which constitutes the most abundant FFA in PS20, were spiked into buffered solutions containing 0.01–0.5 mg/mL intact PS20, mimicking conditions in partially hydrolyzed PS20. As shown in Figure S2A, the gradual addition of FFAs to solutions comprising reduced amounts of intact PS20 (to mimic higher degradation levels) decreased the surface tension in a similar manner as the enzymatically-degraded PS20. Moreover, it was shown that there is a

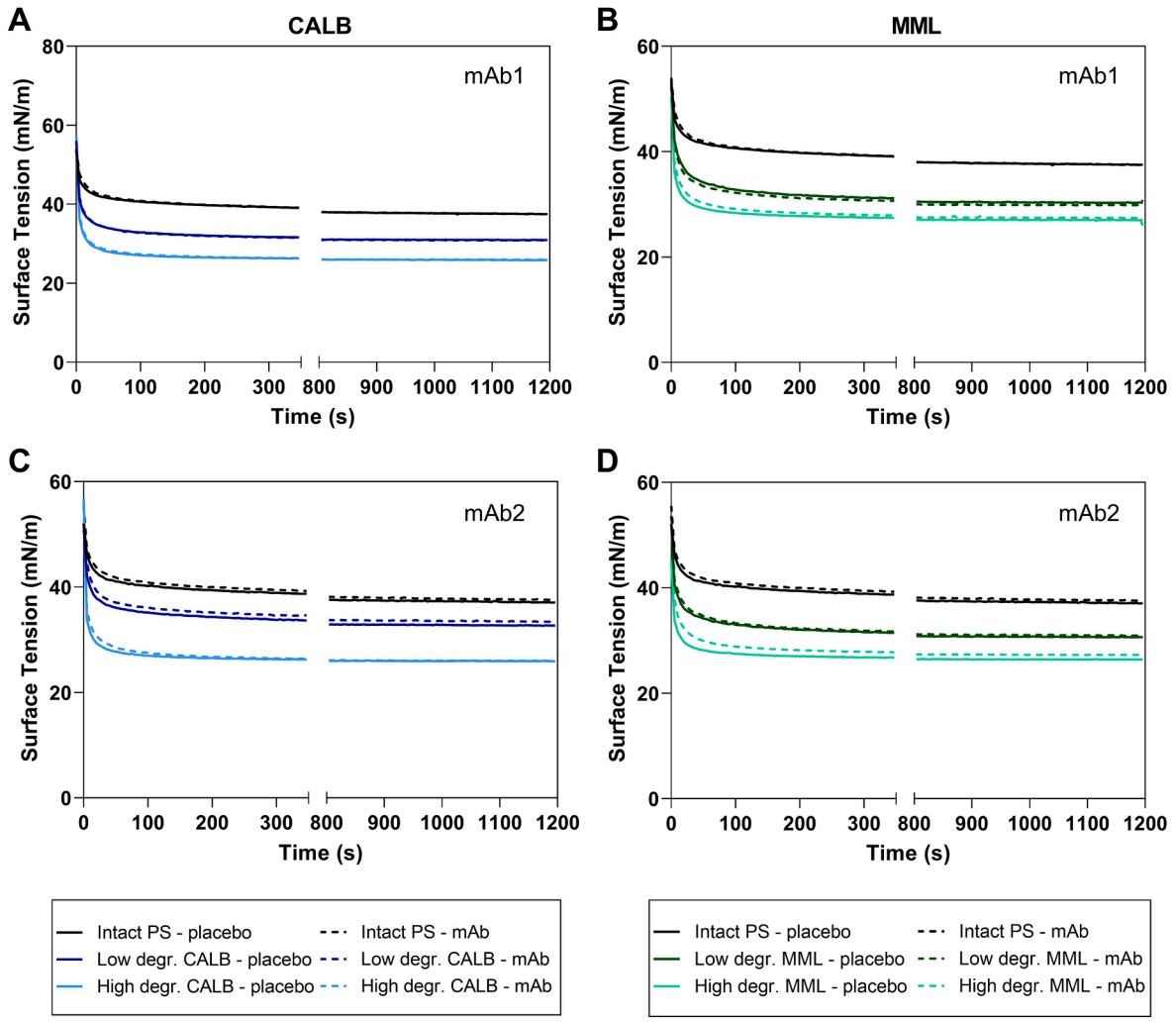

Fig. 4. Equilibrium surface tension of intact and degraded PS20 solutions. Solutions containing either mAb1 (A + B, dotted lines) or mAb2 (C + D, dotted lines) and PS20 degraded by CALB (left) or MML (right), compared to corresponding placebo solutions (solid lines).

threshold around 0.05 mg/mL at which PS20 "degradation" exceeding 40 % will result in a significant increase in surface tension. Taken together, these findings indicate that the minimum concentration of intact PS20 to maintain a sufficiently high interfacial coverage and thus, low surface tension, is around 0.03 mg/mL. However, surface activity of LA in the absence of PS20 (forming a monolayer) was determined to be minor (46.8 mN/m and 54.3 mN/m at respectively 15 µg/mL and 7.6 µg/mL of LA, cf. Fig. S2). These effects seem to corroborate the above co-adsorption assumption, that the surface tension is mainly dictated by intact PS20 but can be further reduced once a mixed layer with LA is formed.

To determine whether there is a displacement of the PS20 by LA or if LA co-adsorbs onto the interface, a buffer exchange experiment was performed. After equilibration, the surface tension was measured while the buffer was gradually exchanged from a buffer system containing either 0.5 mg/mL intact PS20, 0.1 mg/mL intact PS20 and 0.06 mg/mL FFA (mimicking 80 % PS20 degradation), or 0.1 mg/mL intact PS20 without FFA, to a surfactant-free buffer system. This set-up allows for the time-dependent gradual depletion of bulk PS20 and LA molecules and possibly also a partial extraction of the molecules from the air–water interface. As shown in Figure S3, the surface tension of the PS20/FFA mixtures after buffer exchange approximates the surface tension of the PS20 alone at the corresponding concentration, suggesting that LA is gradually removed from the interface. These results support the hypothesis that LA is initially not replacing PS20 but rather intercalating into the PS20 surface layer.

The adsorption of mAbs and intact or partially-degraded surfactants directly after formation of the air–water interface was investigated using the maximum bubble pressure method [6,58]. As depicted in Fig. 5, the surface tension of pure mAb solution (formulation w/o surfactant) was consistently higher than the surface tension of samples comprising surfactant (w/ and w/o mAb). Moreover, the surface tension was rapidly reduced in the presence of intact PS20 or PS20 partially degraded by MML (depletion of HOE species), indicating that the *de novo* liquid–air surface was immediately occupied by intact PS20 or residual monoester species. The tested mAbs showed a different surface tension profile – while the surface tension of mAb1 stayed rather constant over of time (0–5 s), the surface tension of mAb2 declined with a similar slope as the PS20 spiked samples.

Interestingly, both mAb samples supplemented with CALB-degraded PS20 (depletion of monoester species) showed a completely different surface tension profile. Following a lag phase of approximately 0.1–0.5 s, the surface tension temporarily approached the values of pure mAb solution before it rapidly decayed. This observation was not made for corresponding placebo solutions, which exhibited an instant reduction in surface tension directly after the formation of the new interface.

Zoeller et al. [6] have made a similar observation when they tested the dynamic surface tension of bovine serum albumin (BSA) with different surfactants, i.e. PS80, poloxamer 188 (Px188), 2(-hydroxypropyl-)β-cyclodextrin (HPβCD) and trehalose 6-dodecanoate (THDD).

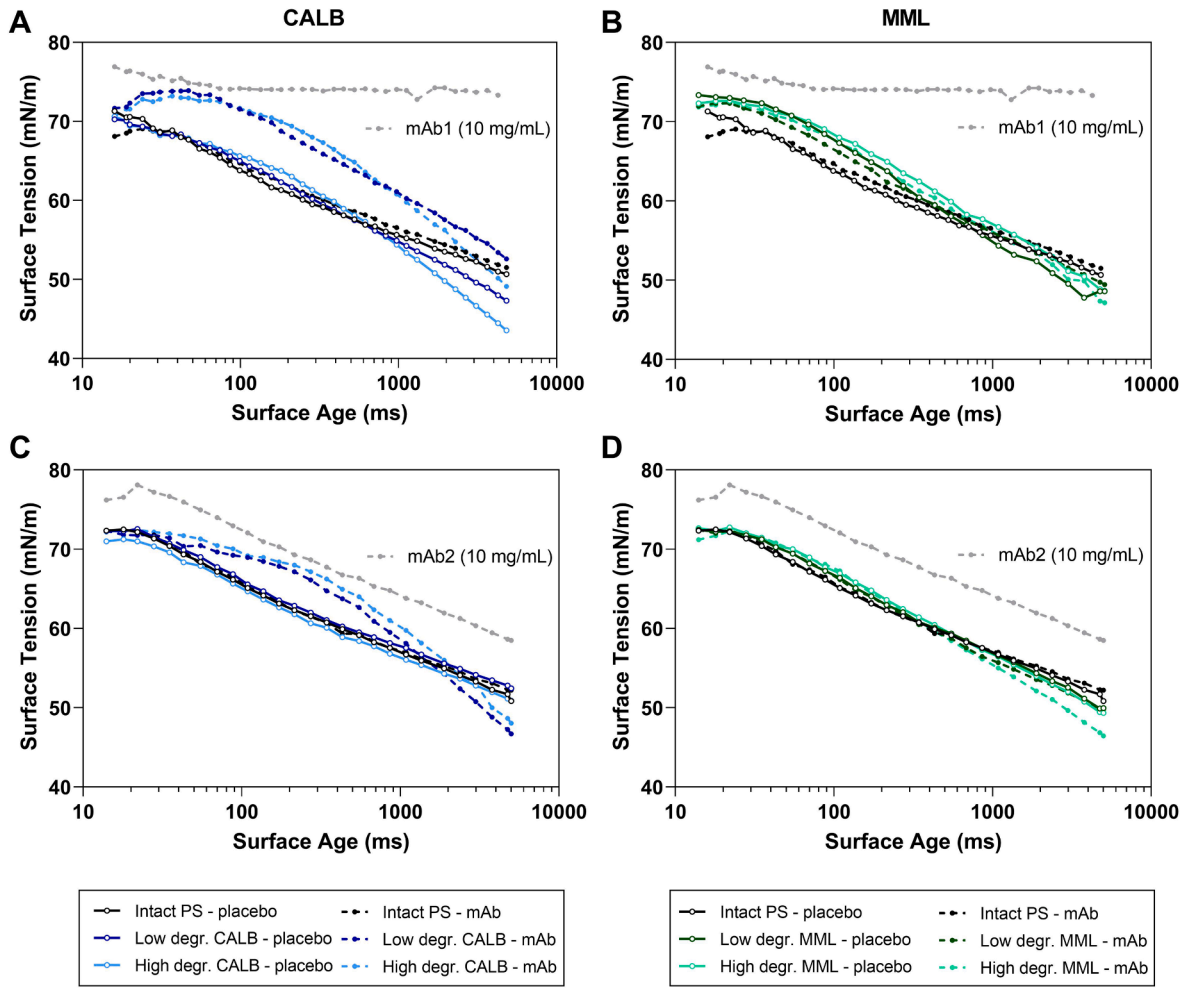

Fig. 5. Dynamic surface tension measurements of mAb1 (A + B, dotted lines) and mAb2 (C + D, dotted lines) supplemented with 0.4 mg/mL PS20 partially degraded by CALB (left) or MML (right), compared to corresponding placebo solutions (solid lines) and pure mAb solutions (gray dotted lines).

They hypothesized that a coincidence of surface tension curves of surfactant–protein and corresponding pure surfactant mixtures suggest that the surfactant is capable to displace the protein from the interface, whereas co-adsorption of protein and surfactant is more likely if the surface tension of the surfactant–protein solutions is higher compared to corresponding surfactant solutions.

As the surface tension of our mAb samples supplemented with CALB-degraded PS20 rapidly declined after the lag phase, we rather believe that these surface tension profiles are caused by a short-term interaction between HOE PS20 components and mAb molecules in the bulk solution, resulting in a delayed diffusion of surface active molecules to the newly formed water–air interface.

In addition, as the hydrophobicity as well as the density of the *de novo* formed interfacial layer depends on the molecular composition, different delays in surface tension decline might be caused by the different time scales of molecular rearrangement processes at the liquid–air interface, i.e. diffusion, intercalation and back-diffusion of surface active molecules (mAbs, FFAs, monoester and HOE species). It needs to be noted that HOE-mAb interactions likely depend on the overall hydrophobicity of mAb molecules and/or the presence of hydrophobic patches on the mAb surface and might be more or less pronounced for different type of mAbs.

Agitation stress experiments.

To investigate whether these differences in dynamic surface tension between CALB and MML degraded PS20 samples correlate with different mAb protective properties against interfacial stress, an agitation stress study was performed. This study assessed the formation of soluble aggregates, sub-visible particles and visible particles. Only mAb1 was used for the agitation stress study because both mAb1 and mAb2 showed a similar change in their dynamic surface tension profile once formulated with CALB-degraded PS20 (Fig. 5). For this purpose, mAb1 formulations were spiked with either intact or partially degraded PS20 (0.4 mg/mL), filled into 6 cc vials and subjected to horizontal shaking stress for 7 days at 25 °C. Vials which were statically stored at 25 °C, as well as one additional vial which was formulated with intact PS20 and subsequently stored at −80 °C, were used as references.

Size exclusion chromatography was used to quantify the increase of soluble aggregates (HMWS).

As depicted in Fig. 6A, neither the unstressed controls (statically stored at 25 °C), nor reference samples containing intact PS20 showed an increase in HMWS, compared to the initial sample (-80 °C reference). By contrast, samples spiked with highly degraded PS20 showed an increase in HMWS after being subjected to agitation stress. While the increase of HMWS in samples containing highly MML-degraded PS20 was only minor (from 0.2 % to 0.4 %), HMWS in CALB-degraded PS20 samples at equal degradation levels showed a significant increase from 0.2 % to 16.6 %, comprising mainly higher-order antibody aggregates (HMW4, cf. Fig. 6B).

These results indicate that monoester components in PS20 are essential for the protection of the tested mAb against interfacial stress and that the depletion of these species eventually result in the formation of soluble aggregates while degradation of HOE species has no

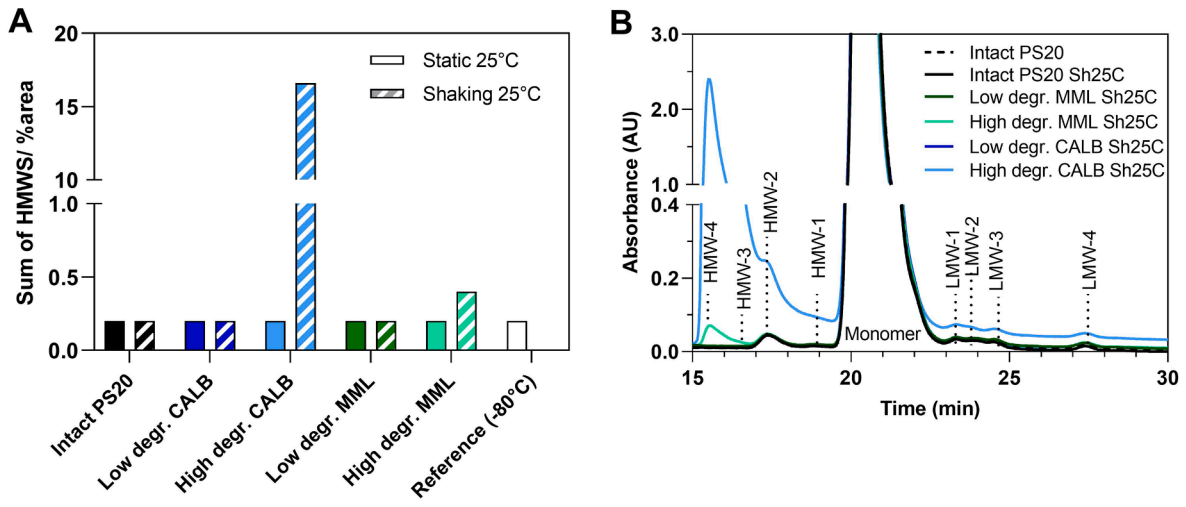

Fig. 6. (A) Sum of HMWS and (B) corresponding SEC chromatograms of unstressed (static 25 °C) and agitated (shaking 25 °C) samples. Soluble mAb aggregates were substantially increased in stressed samples formulated with highly CALB-degraded PS20, whereas corresponding MML samples displayed a slight increase in HMWS.

significant impact on protein aggregation. However, additional studies are needed to 1) investigate the mechanism of protection and 2) systematically test a variety of different mAbs as the stabilizing effects of PS20 subspecies might be altered for different protein formats and/or formulation compositions.

As described earlier, agitation stress experiments were carried out at a lower protein concentration of 1 mg/mL, hence representing a surfactant to mAb ratio that is 10-fold lower relative to the surface tension experiments. This difference must be taken into consideration for interpreting the results and constitutes a possible explanation why the content of HMWS was not increased in low-degradation CALB PS20 containing samples.

Visible particles were assessed by enhanced visual inspection, using a Seidenader V90-T vial inspection machine as well as by the visual method described in the pharmacopeias (Ph.Eur. and USP). No visible particles were observed during the initial visual inspection directly after compounding. As shown in Table 1, samples formulated with intact or partially CALB- or MML-degraded PS20 at low degradation levels were free from visible particles, even after shaking stress. However, visible particles were detected in unstressed and agitated samples containing highly degraded PS20 (CALB and MML). While single discrete particles were found in stressed samples formulated with highly MML-degraded PS20, corresponding CALB-degraded samples had a turbid appearance, indicating a high particle load in these samples. As the high particle load in these samples was only observed by enhanced visual inspection (2-fold magnification) and not by the compendial method (without magnification), it can be assumed that the size of these particles was slightly below the visible threshold. Surprisingly, none of the samples contained significant amounts of sub-visible particles (less than 1000 particles/ mL $\geq$ 2 µm; sub-visible particles $\geq$ 10 µm and $\geq$ 25 µm far below the compendial limits), as determined by light obscuration (Fig. S4).

Particle identification (ID) of selected samples (unstressed and stressed samples with high degradation levels) was investigated by FTIR (Fig. S5), after isolation of sub-visible and visible particles on a gold filter. As shown in Table 2, particles comprising mainly FFAs, as well as one protein particle, were found in unstressed CALB-degraded samples, while many proteinaceous but no FFA particles were detected in corresponding stressed samples. These results suggest that FFA particles were disrupted upon shaking stress, while the number of proteinaceous particles significantly increased in these samples. By contrast, only FFA particles were found in samples containing MML-degraded PS20, which could still be detected after shaking. As the number of FFA particles was extremely high in these samples, it cannot be excluded that potential

Table 1
Visible particle observations in mAb1 samples containing either non-degraded PS20 or surfactant degraded with CALB or MML at two degradation levels. Drug product formulations were assessed for visible particles upon static storage at 25 °C (unstressed) or shaking at 25 °C. Three glass vials per formulation were visually inspected for visible particles according to the Ph. Eur./USP method (top) and with enhanced visual inspection using the Seidenader V90-T vial inspection machine (bottom). Numbers provide an estimate as visual inspection is not a validated method for particle quantification.

Polysorbate 20			**Visible Particles (acc. to Ph.Eur.)**					
			unstressed			**shaking at 25 °C**		
Nominal Conc.	**Degradation**	**Enzyme**	#1	#2	#3	#1	#2	#3
0.4 mg/mL	–	–	0	0	0	0	0	0
	low	CALB	0	0	0	0	0	0
		MML	0	0	0	0	0	0
	high	CALB	0	0	6	>7*	>7*	>7*
		MML	2	0	0	>7	0	0
Polysorbate 20			**Visible Particles (Seidenader)**					
			unstressed			**shaking at 25°C**		
Nominal Conc.	**Degradation**	**Enzyme**	#1	#2	#3	#1	#2	#3
0.4 mg/mL	–	–	0	0	0	0	0	0
	low	CALB	0	0	0	0	0	0
		MML	0	0	0	0	0	0
	high	CALB	>10	>10	>10	>10*	>10*	>10*
		MML	>10	>10	>10	>10	>10	>10

* turbid solution

Table 2
Particle ID results of selected samples analyzed by FTIR. Particles were isolated on a gold filter and washed thoroughly with cold water before FTIR analysis. Spectra were compared against a library and best matches were reported (Fig. S5). Intrinsic particles (e.g. filter fibers or rubber stopper particulates) were excluded from the evaluation.

Sample	Degradation level	Stress condition	Particle ID	
			FFA	Protein
CALB	High	unstressed	67 particles	1 particle
	High	stressed	–	82 particles
MML	High	unstressed	layer	–
	High	stressed	layer	–

protein or FFA/protein particles were masked by FFAs in these samples.

These results complement our findings from the surface tension experiments and confirm that monoester degradation in PS20 plays a pivotal role in the formation of soluble and insoluble (visible) protein aggregates. Moreover, degradation of PS20 by MML enhances the formation of FFA particles, which is mainly by depletion of species with lower CMC (HOE), as well as the release of higher amounts of FFA molecules per surfactant molecule compared to CALB degradation (approx. 1.3-fold higher FFA levels in MML samples, cf. Fig. S6).

Tomlinson et al. [24] found that different monoester species in PS20 are not equally protective against mechanically induced interfacial stress. While isosorbide-POE-monolaurate and POE-monolaurate exhibited superior protection against particle formation, 10-fold higher concentrations of sorbitan-POE-monolaurate were required to achieve the same effect. In our CALB-degraded samples these three monoester species were similarly degraded (cf. Fig. 1A), therefore, no differentiated assessment can be made with regard to the stabilizing properties of one distinct PS20 monoester subspecies.

Interestingly, in their studies, sorbitan-POE-dilaurate was also highly efficient in protecting a model mAb against interfacial stress upon agitation. However, this particular finding could not be confirmed by a recent study from Diederichs et al. [43], who also used fractionated all-laurate PS20 and performed 3D shaking stress experiments with two different mAbs. Their findings suggest that, in contrast to monoester subspecies, HOE species are more prone to particle formation upon mechanically-induced interfacial stress. However, it should be noted that the major experimental differences between the two studies may lead to different results, e.g. differences regarding PS20 fractions, model mAbs, buffer composition and type of shaking stress. In our studies, samples comprising high amounts of HOE (i.e. CALB-degraded samples) performed worse with regard to stabilization upon shaking, which is in line with the recent findings by Diederichs and coworkers. One similarity between the study presented here and the setup used by Diederichs et al. was the use of formulation buffer, in contrast to the study from Tomlinson et al. in which 0.9 % saline solution was used. As different sample solutions have been demonstrated to change the CMC of surfactant molecules [59], it can be expected that different outcomes with regard to the sorbitan-POE-dilaurate fraction might stem from differences in the sample solution composition. In the present study, the degraded PS20 samples contained all components of PS20, but at varying monoester to HOE ratios and with respective degradation products, i.e. fatty acids. It can be assumed that the presence of FFAs changes the behavior of monoester and HOE components in aqueous mAb solution. For example, lower amounts of intact surfactant molecules might be available for saturating the surface. This results from the fact that there is an increased thermodynamically-driven shift of surfactant molecules from the interface into the solution to encapsulate hydrophobic fatty acids into surfactant micelles, or, to form surfactant coated FFA nanoparticles if their solubility limit is exceeded. In addition, depending on the pH, charged FFAs can intercalate into the liquid–air interface, forming mixed surfactant layers which can be more densely packed compared to layers without FFAs [60]. A very similar approach to our study was very recently published by Glücklich et al. [44]. In contrast to the previous papers discussed above, Glücklich and coworkers used non-immobilized lipases with different PS20 substrate specificity to generate PS20 degradation profiles which were more representative of end-of-shelf life drug product. They found that preferential degradation of monoesters resulted in the highest protein stabilization effect with regard to interfacial stress, whereas HOE degradation and equal degradation of all PS20 ester species (monoester and HOE) resulted in a significantly reduced stabilization. These outcomes contradict our observation that preferential HOE degradation does not have a major impact on formulation stability, whereas monoester degradation resulted in altered dynamic surface tension properties and, eventually, enhanced the formation of HMWS and visible particles in a mAb formulation upon shaking stress. Again, a direct comparison between their study and the present one is difficult due to differences in the experimental setup. As shown by Tomlinson et al. [24] and Diederichs et al. [43], distinct components in PS20 may possess superior protective effects (i.e. isosorbide-PEO-monolaurate), while it can be interpreted that others (i.e. sorbitan-PEO-monolaurate) might not significantly contribute to the protection against agitation stress. Therefore, and even if the ratio of monoester and HOE is similar, interfacial protection might be slightly altered. In addition, in our study the most significant differences between HOE and monoester degradation were observed at the high PS degradation level corresponding to 55–60 % hydrolysis, whereas Glücklich et al. [44] studied effects at a degradation level of 20 %. Another difference, however, was the preparation process of enzymatically hydrolyzed PS samples. While we used bead-immobilized enzymes, which were removed once the desired degradation level was reached, Glücklich et al. used soluble enzymes, which were directly spiked into the PS20 stock solutions. In their study, PS degradation was stopped by heat inactivation and mixtures of both heat-inactivated degraded and non-degraded PS were used to prepare 20 % degraded PS20 solutions. Even though this approach is deemed more representative compared to isolated PS20 ester fractions, commercially available enzymes are usually offered at 95–98 % purity. Therefore, the use of soluble enzymes, which were heat-inactivated but not removed or further purified, may lead to the introduction of impurities that potentially impair protein stability.

Fatty acids have recently been reported to induce protein aggregation. Zhang et al. [61] concluded that presence of oleic acid (OA) poses a higher risk for the formation of proteinaceous particles in mAb formulations as compared to LA. However, most of their data was generated in the absence of intact PS20 which is not representative of long-term drug stability studies and the corresponding observations of higher solubility of LA over OA in formulation buffer contradicts findings elsewhere [18]. Zhang et al. also reported that FFA induced protein particle formation could be fully mitigated by the presence of 0.1 mg/mL PS20. Hence, it is not expected that the formation of proteinaceous particles was enhanced by FFAs in our experiments, especially since the concentration of FFAs was slightly higher in MML samples, compared to corresponding CALB samples (Fig. S4) and the concentration of residual intact PS20 was always above 0.1 mg/mL in samples used for the shaking stress study.

4. Conclusions

The aim of this work was to gain a more comprehensive understanding on how different enzymatic PS20 degradation patterns impact interfacial properties, and thereby, stability of liquid biopharmaceutical formulations. In essence, degradation of PS20 HOE, as observed for MML, results in a higher risk for FFA particle formation while PS20 monoester depletion increases the risk for the generation of protein particles. As a consequence, the different enzymes or mixtures thereof - which may be present in drug substance and drug product - considerably impact stability. Further studies are necessary to elucidate all underlying mechanisms for the observations, e.g., how monoester degradation impairs mAbs stability. As the current results partially stand in contrast with findings by other research groups, the impact of the enzymatic

PS20 degradation profile on agitation protection should be systematically investigated using a higher number of mAbs of different formats. In summary, this study provides valuable insights on the interplay of different PS degradation products at formulation interfaces that should be considered during biopharmaceutical product development.

Declaration of Competing Interest

The authors declare that they have no known competing financial interests or personal relationships that could have appeared to influence the work reported in this paper.

Data availability

Data will be made available on request.

Acknowledgements

The authors would like to acknowledge Christoph Paschen and Berk Kocar (Analytical Development, F. Hoffmann-La Roche Ltd.) for supporting the polysorbate analysis, Christian Reisen (Formulation and Processing Development, F. Hoffmann-La Roche Ltd.) for performing the SEC analysis and Christiane Hess (Formulation and Processing Development, F. Hoffmann-La Roche Ltd.) for performing the FTIR measurements. Furthermore, the authors would like to thank Inn Yuk, Nidhi Doshi (Pharma Technical Development US, Genentech Inc.), Lisa Dietel, Nuria Sancho-Oltra, Denis Klemm and Cosimo Pinto (Pharma Technical Development Europe, F. Hoffmann-La Roche Ltd.) for feedback and discussions.

Appendix A. Supplementary data

Supplementary data to this article can be found online at https://doi.org/10.1016/j.ejpb.2023.11.024.

References

[1] A. Kannan, I.C. Shieh, P. Hristov, G.G. Fuller, In-use interfacial stability of monoclonal antibody formulations diluted in saline i.v. bags, J. Pharm. Sci. 110 (2021) 1687–1692.
[2] A. Kannan, I.C. Shieh, D.L. Leiske, G.G. Fuller, Monoclonal antibody interfaces: Dilatation mechanics and bubble coalescence, Langmuir the ACS J. Surfaces and Colloids. 34 (2018) 630–638.
[3] T.A. Khan, H.-C. Mahler, R.S.K. Kishore, Key interactions of surfactants in therapeutic protein formulations: A review, European J. Pharmaceutics and Biopharmaceutics Official J. Arbeitsgemeinschaft Fur Pharmazeutische Verfahrenstechnik E.v. 97 (2015) 60–67.
[4] T.A. Khan, D.C. Gomes, C. Grapentin, M. Heitz, C. Mueller, Mechanisms of stabilization of proteins by surfactants, in: Surfactants in biopharmaceutical development, Elsevier. (2023) 59–102, https://doi.org/10.1016/B978-0-12-812503-8.00004-X.
[5] E. Koepf, R. Schroeder, G. Brezesinski, W. Friess, The film tells the story: Physical-chemical characteristics of IgG at the liquid-air interface, European J. Pharmaceutics and Biopharmaceutics Official J. Arbeitsgemeinschaft Fur Pharmazeutische Verfahrenstechnik E.v 119 (2017) 396–407.
[6] M.P. Zoeller, S. Hafiz, A. Marx, N. Erwin, G. Fricker, J.F. Carpenter, Exploring the protein stabilizing capability of surfactants against agitation stress and the underlying mechanisms, J. Pharm. Sci. 111 (2022) 3261–3274.
[7] I.C. Shieh, A.R. Patel, Predicting the agitation-induced aggregation of monoclonal antibodies using surface tensiometry, Mol. Pharm. 12 (2015) 3184–3193.
[8] J.S. Bee, T.W. Randolph, J.F. Carpenter, S.M. Bishop, M.N. Dimitrova, Effects of surfaces and leachables on the stability of biopharmaceuticals, J. Pharm. Sci. 100 (2011) 4158–4170.
[9] J.F. Carpenter, T.W. Randolph, W. Jiskoot, D.J.A. Crommelin, C.R. Middaugh, G. Winter, Y.-X. Fan, S. Kirshner, D. Verthelyi, S. Kozlowski, K.A. Clouse, P. G. Swann, A. Rosenberg, B. Cherney, Overlooking subvisible particles in therapeutic protein products: Gaps that may compromise product quality, J. Pharm. Sci. 98 (2009) 1201–1205.
[10] H.J. Lee, A. McAuley, K.F. Schilke, J. McGuire, Molecular origins of surfactant-mediated stabilization of protein drugs, Adv. Drug Deliv. Rev. 63 (2011) 1160–1171.
[11] M.T. Jones, H.-C. Mahler, S. Yadav, D. Bindra, V. Corvari, R.M. Fesinmeyer, K. Gupta, A.M. Harmon, K.D. Hinds, A. Koulov, W. Liu, K. Maloney, J. Wang, P. Y. Yeh, S.K. Singh, Considerations for the use of polysorbates in biopharmaceuticals, Pharm. Res. 35 (2018) 148.
[12] European Directorate for the Quality of Medicines, Monograph Polysorbate 20 [01/2017:0426], European Pharmacopeia 10.0 2020.
[13] United States Pharmacopeia and National Formulary, NF Monographs, Polysorbate 20, United States Pharmacopeia 2020.
[14] A.M. Morales, A. Sreedhara, J. Buecheler, S. Brosig, D. Chou, T. Christian, T. Das, I. de Jong, J. Fast, B. Jagannathan, E.M. Moussa, M.R. Nejadnik, I. Prajapati, A. Radwick, Y. Rahman, S. Singh, End-to-End approach to surfactant selection, risk mitigation, and control strategies for protein-based therapeutics, AAPS J. 25 (2022) 6.
[15] K. Wuchner, L. Yi, C. Chery, F. Nikels, F. Junge, G. Crotts, G. Rinaldi, J.A. Starkey, K. Bechtold-Peters, M. Shuman, M. Leiss, M. Jahn, P. Garidel, R. de Ruiter, S. M. Richer, S. Cao, S. Peuker, S. Huille, T. Wang, V. Le Brun, Industry perspective on the use and characterization of polysorbates for biopharmaceutical products part 1: Survey report on current state and common practices for handling and control of polysorbates, J. Pharm. Sci. 111 (2022) 1280–1291.
[16] K. Wuchner, L. Yi, C. Chery, F. Nikels, F. Junge, G. Crotts, G. Rinaldi, J.A. Starkey, K. Bechtold-Peters, M. Shuman, M. Leiss, M. Jahn, P. Garidel, R. de Ruiter, S. M. Richer, S. Cao, S. Peuker, S. Huille, T. Wang, V. Le Brun, Industry perspective on the use and characterization of polysorbates for biopharmaceutical products part 2: Survey report on control strategy preparing for the future, J. Pharm. Sci. 111 (2022) 2955–2967.
[17] N. Doshi, B. Demeule, S. Yadav, Understanding particle formation: Solubility of free fatty acids as polysorbate 20 degradation byproducts in therapeutic monoclonal antibody formulations, Mol. Pharm. 12 (2015) 3792–3804.
[18] N. Glücklich, M. Dwivedi, S. Carle, J. Buske, K. Mäder, P. Garidel, An in-depth examination of fatty acid solubility limits in biotherapeutic protein formulations containing polysorbate 20 and polysorbate 80, Int. J. Pharm. 591 (2020) 119934.
[19] N. Doshi, R. Fish, K. Padilla, S. Yadav, Evaluation of super refined™ polysorbate 20 with respect to polysorbate degradation, particle formation and protein stability, J. Pharm. Sci. 109 (2020) 2986–2995.
[20] A. Tomlinson, B. Demeule, B. Lin, S. Yadav, Polysorbate 20 degradation in biopharmaceutical formulations: Quantification of free fatty acids, characterization of particulates, and insights into the degradation mechanism, Mol. Pharm. 12 (2015) 3805–3815.
[21] M. Dwivedi, M. Blech, I. Presser, P. Garidel, Polysorbate degradation in biotherapeutic formulations: Identification and discussion of current root causes, Int. J. Pharm. 552 (2018) 422–436.
[22] R.S.K. Kishore, S. Kiese, S. Fischer, A. Pappenberger, U. Grauschopf, H.-C. Mahler, The degradation of polysorbates 20 and 80 and its potential impact on the stability of biotherapeutics, Pharm. Res. 28 (2011) 1194–1210.
[23] R.S.K. Kishore, A. Pappenberger, I.B. Dauphin, A. Ross, B. Buergi, A. Staempfli, H.-C. Mahler, Degradation of polysorbates 20 and 80: Studies on thermal autoxidation and hydrolysis, J. Pharm. Sci. 100 (2011) 721–731.
[24] A. Tomlinson, I.E. Zarraga, B. Demeule, Characterization of polysorbate ester fractions and implications in protein drug product stability, Mol. Pharm. 17 (2020) 2345–2353.
[25] I.H. Yuk, T. Koulis, N. Doshi, K. Gregoritza, C. Hediger, V. Lebouc-Haefliger, J. Giddings, T.A. Khan, Formulation mitigations for particle formation induced by enzymatic hydrolysis of polysorbate 20 in protein-based drug products: Insights from a full-factorial longitudinal study, AAPS Open. 8 (2022).
[26] B. Kozuch, J. Weber, J. Buske, K. Mäder, P. Garidel, T. Diederichs, Comparative stability study of polysorbate 20 and polysorbate 80 related to oxidative degradation, Pharmaceutics. 15 (2023).
[27] N.R. Larson, Y. Wei, I. Prajapati, A. Chakraborty, B. Peters, C. Kalonia, S. Hudak, S. Choudhary, R. Esfandiary, P. Dhar, C. Schöneich, C.R. Middaugh, Comparison of polysorbate 80 hydrolysis and oxidation on the aggregation of a monoclonal antibody, J. Pharm. Sci. 109 (2020) 633–639.
[28] J. Weber, J. Buske, K. Mäder, P. Garidel, T. Diederichs, Oxidation of polysorbates - An underestimated degradation pathway? Int. J. Pharmaceutics: X. 6 (2023) 100202.
[29] E.V. Brovč, S. Pajk, R. Šink, J. Mravljak, Protein Formulations Containing Polysorbates: Are Metal Chelators Needed at All? Antioxidants 9 (2020) 441, https://doi.org/10.3390/antiox9050441.
[30] A. Schmidt, A. Koulov, J. Huwyler, H.-C. Mahler, M. Jahn, Stabilizing polysorbate 20 and 80 against oxidative degradation, J. Pharm. Sci. 109 (2020) 1924–1932.
[31] S.K. Gupta, T. Graf, F.T. Edelmann, H. Seelmann, M. Reintinger, L. Hillringhaus, F. Bergmann, M. Wiedmann, R. Falkenstein, H. Wegele, I.H. Yuk, M. Leiss, A fast and sensitive high-throughput assay to assess polysorbate-degrading hydrolytic activity in biopharmaceuticals, European J. Pharmaceutics and Biopharmaceutics Official J. Arbeitsgemeinschaft Fur Pharmazeutische Verfahrenstechnik E.v. 187 (2023) 120–129.
[32] N. Dixit, N. Salamat-Miller, P.A. Salinas, K.D. Taylor, S.K. Basu, Residual host cell protein promotes polysorbate 20 degradation in a sulfatase drug product leading to free fatty acid particles, J. Pharm. Sci. 105 (2016) 1657–1666.
[33] T. Hall, S.L. Sandefur, C.C. Frye, T.L. Tuley, L. Huang, Polysorbates 20 and 80 degradation by group XV lysosomal phospholipase A2 Isomer X1 in monoclonal antibody formulations, J. Pharm. Sci. 105 (2016) 1633–1642.
[34] T. Graf, A. Tomlinson, I.H. Yuk, R. Kufer, B. Spensberger, R. Falkenstein, A. Shen, H. Li, D. Duan, W. Liu, S. Wohlrab, F. Edelmann, M. Leiss, Identification and characterization of polysorbate-degrading enzymes in a monoclonal antibody formulation, J. Pharm. Sci. 110 (2021) 3558–3567.
[35] N. Doshi, J. Martin, A. Tomlinson, Improving prediction of free fatty acid particle formation in biopharmaceutical drug products: Incorporating ester distribution during polysorbate 20 degradation, Mol. Pharm. 17 (2020) 4354–4363.

[36] J.H. Park, J.H. Jin, M.S. Lim, H.J. An, J.W. Kim, G.M. Lee, Proteomic analysis of host cell protein dynamics in the culture supernatants of antibody-producing CHO cells, Sci. Rep. 7 (2017) 44246.
[37] J. Chiu, K.N. Valente, N.E. Levy, L. Min, A.M. Lenhoff, K.H. Lee, Knockout of a difficult-to-remove CHO host cell protein, lipoprotein lipase, for improved polysorbate stability in monoclonal antibody formulations, Biotechnol. Bioeng. 114 (2017) 1006–1015.
[38] S. Zhang, H. Xiao, R. Molden, H. Qiu, N. Li, Rapid polysorbate 80 degradation by liver carboxylesterase in a monoclonal antibody formulated drug substance at early stage development, J. Pharm. Sci. 109 (2020) 3300–3307.
[39] A.C. McShan, P. Kei, J.A. Ji, D.C. Kim, Y.J. Wang, Hydrolysis of polysorbate 20 and 80 by a range of carboxylester hydrolases, PDA J. Pharm. Sci. Technol. 70 (2016) 332–345.
[40] T. Graf, K. Abstiens, F. Wedekind, C. Elger, M. Haindl, C. Wurth, M. Leiss, Controlled polysorbate 20 hydrolysis - A new approach to assess the impact of polysorbate 20 degradation on biopharmaceutical product quality in shortened time, Eur. J. Pharm. Biopharm. 152 (2020) 318–326.
[41] C. Vaclaw, K. Merritt, V.P. Griffin, N. Whitaker, M. Gokhale, D.B. Volkin, M. O. Ogunyankin, P. Dhar, Comparison of protein particle formation in IgG1 mAbs formulated with PS20 Vs. PS80 when subjected to interfacial dilatational stress, AAPS PharmSciTech. 24 (2023) 104.
[42] Y. Wang, T. Wang, Q. Chen, W. Zhou, J. Guo, Correlation between the protein pharmaceutical surface activity and interfacial stability, Mol. Pharm. 20 (2023) 2536–2544.
[43] T. Diederichs, J.J. Mittag, J. Humphrey, S. Voss, S. Carle, J. Buske, P. Garidel, Existence of a superior polysorbate fraction in respect to protein stabilization and particle formation? Int. J. Pharm. 635 (2023) 122660.
[44] N. Glücklich, S. Carle, T. Diederichs, J. Buske, K. Mäder, P. Garidel, How enzymatic hydrolysis of polysorbate 20 influences colloidal protein stability, Eur. J. Pharm. Sci. (2023) 106597.
[45] V.S. Nayak, Z. Tan, P.M. Ihnat, R.J. Russell, M.J. Grace, Evaporative light scattering detection based HPLC method for the determination of polysorbate 80 in therapeutic protein formulations, J. Chromatogr. Sci. 50 (2012) 21–25.
[46] D. Hewitt, T. Zhang, Y.-H. Kao, Quantitation of polysorbate 20 in protein solutions using mixed-mode chromatography and evaporative light scattering detection, J. Chromatogr. A. 1215 (2008) 156–160.
[47] Y. Li, D. Hewitt, Y.K. Lentz, J.A. Ji, T.Y. Zhang, K. Zhang, Characterization and stability study of polysorbate 20 in therapeutic monoclonal antibody formulation by multidimensional ultrahigh-performance liquid chromatography-charged aerosol detection-mass spectrometry, Anal. Chem. 86 (2014) 5150–5157.
[48] M.N. Honemann, J. Wendler, T. Graf, A. Bathke, C.H. Bell, Monitoring polysorbate hydrolysis in biopharmaceuticals using a QC-ready free fatty acid quantification method, J. Chromatogr. B, Analytical Technol. in the Biomedical and Life Sci. 1116 (2019) 1–8.
[49] R.M. Brito, W.L. Vaz, Determination of the critical micelle concentration of surfactants using the fluorescent probe N-phenyl-1-naphthylamine, Anal. Biochem. 152 (1986) 250–255.
[50] N. Doshi, K. Ritchie, T. Shobha, J. Giddings, K. Gregoritza, R. Taing, S. Rumbelow, J. Chu, A. Tomlinson, A. Kannan, M. Saggu, S.K. Cai, V. Nicoulin, W. Liu, S. Russell, L. Luis, S. Yadav, Evaluating a modified high purity polysorbate 20 designed to reduce the risk of free fatty acid particle formation, Pharm. Res. (2021).
[51] European Directorate for the Quality of Medicines, Particulate contamination: Visible particles [2.9.20], European Pharmacopeia 10.0 2020.
[52] A. Allmendinger, V. Lebouc, L. Bonati, A. Woehr, R.S.K. Kishore, K. Abstiens, Glass leachables as a nucleation factor for free fatty acid particle formation in biopharmaceutical formulations, J. Pharm. Sci. 110 (2021) 785–795.
[53] D. Ditter, H.-C. Mahler, L. Gohlke, A. Nieto, H. Roehl, J. Huwyler, M. Wahl, A. Allmendinger, Impact of vial washing and depyrogenation on surface properties and delamination risk of glass vials, Pharm. Res. 35 (2018) 146.
[54] European Directorate for the Quality of Medicines, Particulate contamination: Sub-visible particles [2.9.19], European Pharmacopeia 10.0 2020.
[55] P. Shi, H. Zhang, L. Lin, C. Song, Q. Chen, Z. Li, Molecular dynamics simulation of four typical surfactants in aqueous solution, RSC Adv. 9 (2019) 3224–3231.
[56] M. Lapelosa, T.W. Patapoff, I.E. Zarraga, Molecular simulations of micellar aggregation of polysorbate 20 ester fractions and their interaction with N-phenyl-1-naphthylamine dye, Biophys. Chem. 213 (2016) 17–24.
[57] N. Doshi, J. Giddings, L. Luis, A. Wu, K. Ritchie, W. Liu, W. Chan, R. Taing, J. Chu, A. Sreedhara, A. Kannan, P. Kei, I. Shieh, T. Graf, M. Hu, A Comprehensive Assessment of All-Oleate Polysorbate 80: Free fatty acid particle formation, interfacial protection and oxidative degradation, Pharm. Res. 38 (2021) 531–548.
[58] T. Serno, E. Härtl, A. Besheer, R. Miller, G. Winter, The role of polysorbate 80 and HPβCD at the air-water interface of IgG solutions, Pharm. Res. 30 (2013) 117–130.
[59] P. Garidel, M. Blech, J. Buske, A. Blume, Surface tension and self-association properties of aqueous polysorbate 20 HP and 80 HP solutions: Insights into protein stabilisation mechanisms, J Pharm Innov. 16 (2021) 726–734.
[60] A. Kannan, J. Giddings, S. Mehta, T. Lin, A. Tomlinson, K. Ritchie, I. Shieh, M. Saggu, N. Doshi, A mechanistic understanding of monoclonal antibody interfacial protection by hydrolytically degraded polysorbate 20 and 80 under IV bag conditions, Pharm. Res. 39 (2022) 563–575.
[61] J. Zhang, J. He, K.J. Smith, Fatty acids can induce the formation of proteinaceous particles in monoclonal antibody formulations, J. Pharm. Sci. 111 (2022) 655–662.